# Thiol antioxidant-functionalized CdSe/ZnS quantum dots: Synthesis, Characterization, Cytotoxicity

**Hong Zheng**[1], **Luke J. Mortensen**[2], and **Lisa A. DeLouise**[1,2,*]

[1]Department of Dermatology, University of Rochester, Rochester NY, 14642, USA

[2]Department of Biomedical Engineering, University of Rochester, Rochester NY, 14642, USA

## Abstract

Nanotechnology is a growing industry with wide ranging applications in consumer product and technology development. In the biomedical field, nanoparticles are finding increasing use as imaging agents for biomolecular labeling and tumor targeting. The nanoparticle physiochemical properties must be tailored for the specific application but chemical and physical stability in the biological milieu (no oxidation, aggregation, agglomeration or toxicity) are often required. Nanoparticles used for biomolecular fluorescent imaging should also have high quantum yield (QY). The aim of this paper is to examine the QY, stability, and cell toxicity of a series of positive, negative and neutral surface charge quantum dot (QD) nanoparticles. Simple protocols are described to prepare water soluble QDs by modifying the surface with thiol containing antioxidant ligands and polymers keeping the QD core/shell composition constant. The ligands used to produce negatively charged QDs include glutathione (GSH), N-acetyl-L-cysteine (NAC), dihydrolipoic acid (DHLA), tiopronin (TP), bucilliamine (BUC), and mercaptosuccinic acid (MSA). Ligands used to produce positively charged QDs include cysteamine (CYS) and polyethylenimine (PEI). Dithiothreitol (DTT) was used to produce neutral charged QDs. Commercially available nonaqueous octadecylamine (ODA) capped QDs served as the starting material. Our results suggest that QD uptake and cytotoxicity are both dependent on surface ligand coating composition. The negative charged GSH coated QDs show superior performance exhibiting low cytotoxicity, high stability, high QY and therefore are best suited for bioimaging applications. PEI coated QD also show superior performance exhibiting high QY and stability. However, they are considerably more cytotoxic due to their high positive charge which is an advantageous property that can be exploited for gene transfection and/or tumor targeting applications. The synthetic procedures described are straightforward and can be easily adapted in most laboratory settings.

## Introduction

Fluorescent probes are powerful imaging and tracking tools for a wide range of biomedical applications such as disease diagnoses and prognosis, tracking cell/protein interactions, and cell sorting. Traditional organic dyes used in these applications are limited by their short lifetime, narrow excitation range, and low fluorescence intensity. Quantum dots (QDs) are

*Corresponding author: Lisa_DeLouise@urmc.rochester.edu.

fluorescent semiconductor nanoparticles with a typical core size of 2–10 nm. In the past decade the design of QDs for biomedical applications has generated much interest. In comparison with organic dyes, QDs have tunable fluorescence signatures, broad excitation with narrow emission, and superior photostability. These properties have spurred investigation of QDs as fluorescence biomarkers for both static and kinetic in vivo imaging[1–4].

Successful use of QD in biomedical imaging applications requires high brightness and biocompatibility which both depend on the surface coating chemistry. Common QD core/shell synthesis procedures are conducted in organic solvent (e.g. hexane, toluene, cholorform) yielding QDs coated with hydrophobic surface ligands such as trioctylphosphine oxide (TOPO), trioctylphosphine (TOP) and octadecylamine (ODA)[5–7]. Commercially available solvent soluble QD are cost effective to purchase but to be useful for biomedical applications they must be rendered water-soluble. In addition, the water soluble QDs must maintain colloidal stability (i.e., a lack of aggregation/agglomeration) in a biological milieu, they should exhibit low cytotoxicity, and a high quantum yield (QY) is desired.

Several protocols have been developed to prepare water soluble QDs including encapsulation and ligand exchange[8–12]. Silica shell[13] and polymer/phospholipid[14,15] encapsulation methods provide good aqueous solubility and QY but they result in a substantial increase of particle size, which may restrict access to confined biomolecular spaces and prevent renal elimination in vivo application[16]. Ligand exchange using short-chain thiol-based ligands is an attractive approach commonly used that provides a very compact water solubilizing shell around QDs. However, the majority of protocols used to replace TOPO or ODA often require high temperature processing which cause problems of diminished QY and poor colloidal stability in water. Therefore, ligand exchange procedures that can overcome these limitations are in great demand.

The composition of the water solubilizing ligand plays a key role in determining cytotoxicity. The core composition of many semiconductor QDs is comprised of CdSe or CdTe. The presence of Cd raises concern for potential heavy metal toxicity and has restricted human in vivo use[17–20]. Therefore, ligand coatings that can stabilize the QD, minimize degradation and/or counter the toxic effects are of great interest[21–23]. The composition of ligand coating contributes significantly to the QD surface charge which effects particle aggregation/agglomeration (size) and stability against core oxidation[24–27]. Charge and size also affect cellular internalization and processing[24,28]. Hoshino and co-workers reported that the cytotoxicity of CdSe-ZnS core/shell QDs depended more on the physicochemical properties of the coating ligands than the core core/shell composition[21]. Lovric et al. similarly concluded that the physicochemical characteristics of CdTe core QDs influenced subcellular localization and cytotoxicity; quantified as generation of reactive oxygen species (ROS)[28]. The association of ROS with QD induced cytotoxicity has spurred the investigation of antioxidant ligand coatings. For example, Choi et al. demonstrated that negatively charged (−9.8 mV) CdTe core QDs coated with N-acetylcysteine (NAC), a thiol antioxidant, successfully reduced QD cytotoxicity in human neuroblastoma cells quantified by a decrease in membrane lipid peroxidation and mitochondrial impairment relative to

positively charged (+14.2 mV) cysteamine-capped CdTe QDs[18]. However, the observation of reduce cytotoxicity in this study can not be conclusively attributed to antioxidant effect of NAC due to the contrasting surface charge on the QD tested.

In this study we sought to develop simply ligand exchange protocols to produce a charge series (positive, negative, and neutral) of QDs with equivalent core/shell composition and properties that would be useful for biological studies (high QY, stability, low cytotoxicity). We evaluated several thiol containing small molecules with antioxidants properties[29] including glutathione (GSH), N-acetyl-L-cysteine (NAC), dihydrolipoic acid (DHLA), bucilliamine (BUC), cysteamine (CYS), and dithiothreitol (DTT). In addition, we investigated tiopronin (TP), a thiol containing reducing agent used to prevent kidney stone formation by solublizing cystine[30], and two a widely used surface ligands, mercaptosuccinic acid (MSA) and polyethylenimine (PEI). The molecular structures of the ligands investigated are shown in Table 1.

Guided by literature[31–33], we developed modified protocols to exchange the hydrophobic coating on CdSe/ZnS QDs with the water soluble ligands. The ligand-exchange procedures developed are simplified using mild reaction conditions (reduced solution temperature 60 ℃) and an organic base (tetramethylammonium hydroxide) to increase the reactivity of the thiol with ZnS surface. These modifications prevent uncontrolled aggregation during ligand-exchange process. The physicochemical properties (size, charge, QY), biocompatibility, and cytotoxicity of the water soluble ligands produced were characterized. Results find PEI (+) and GSH (−) coated QD exhibit superior stability and optical properties and therefore are well suited for use in biomedical applications investigating, for example, the effect of surface charge on skin penetration or cell uptake – an important property for drug delivery or gene transfection applications. The simple ligand exchange protocols reported can be easily adapted in most laboratory setting providing a cost saving alternative to the purchase of commercial water soluble QDs.

## Results and Discussion

### Formation of negatively and neutral charged thiol-based ligands coated QDs

Reaction conditions were optimized to produce negatively charged water soluble QDs using octadecylamine (ODA) coated QD (NNLabs) as described in the Materials and Methods Section B2. The procedures described can also be used to exchange trioctylphosphine oxide (TOPO) or trioctylphosphine (TOP) ligands which are common hydrophobic coatings produced on commercially available QDs. The bifunctional ligands chosen for this study (Table 1) contain a thiol group to anchor the QD surface via thiolate formation (metal sulfur bond) and a carboxylic acid/hydroxyl group to impart water solubility and a negative/neutral surface charge. To promote surface coupling the ligand-exchange reaction is conducted under basic conditions to insure deprotonation and nucleophilicity of the thiol group (−SH). The pH of ligand solution was adjusted depending upon its pKa. The general procedure begins by precipitating the organic coated QD and resuspending in THF which is a preferred solvent for solubilzing and separating the hydrophobic ligand. The bifunctional ligand is dissolved in methanol; a polar solvent into which the water soluble QDs accumulate. After reacting the QD and bifunctional ligand solutions, the water soluble QDs are recovered by

precipitation. We found that it was convenient to carry out precipitation with ether in a hydrophobic vessel (e.g., polypropylene) where the QD sample is observed as a fluorescent droplet floating on the ether solution. If a glass container is used the QDs adhere to the wall making it difficult to efficiently recover them.

## Measurement of UV/Vis absorption spectra and photoluminescence spectra

We examined the optical characteristics of the QDs by measuring the absorption and fluorescence spectra. Figure 1 shows a comparison of the absorption spectra of QDs capped with different ligands at equivalent molar concentration (8 μM). Small changes in peak absorbance intensity and slight shifts in the peak wavelength are observed. This suggests the quality of QD ZnS shell is sufficient high to protect the core during the ligand exchange protocol. Much larger changes in peak absorption and peak wavelength occur when QDs with inferior shell are modified with the same ligands [Fig 1S].

Figure 2 shows a comparison the photoluminescence (PL) spectra of the QDs capped with different ligands at equivalent molar concentration (8 μM). As observed in the absorption spectra, the PL spectra shape and peak wavelength do not vary significantly with ligand composition. Again this in not observed with all commercially available QDs [Fig. 2S]. However, we do observe that the magnitude of the photoluminescence peak intensity varies over a wide range suggesting a dependence of QY on ligand composition which we quantify next.

## Size, Surface-charge and Quantum yield

Transmission electron microscopy (TEM. Hitachi H-7100) was used to characterize the size, shape, and aggregation state of the ODA-CdSe/ZnS core/shell QD (NNLabs) starting material. Image analysis (Fig. 3) finds well dispersed, spherical QDs with an average particle diameter of $6.55 \pm 1.17$ nm. Dynamic light scattering (DLS) was used to quantify the hydrodynamic diameter (HD) and surface charge (zeta potential) of the water soluble QDs produced. TEM was not performed on the water soluble QD as the synthetic steps only modify the surface chemistry. Results for the various ligands are summarized in Table 2. Raw DLS size and charge data for the GSH-QDs in DI water (pH=6.6) are shown in Figure 3S. The GSH, NAC, DLHA, TP, BUC, and MSA ligands all produce small hydrodynamic diameter QDs (13–28 nm) with strong negative charge (−23 to −34 mV) due to the presence of carboxyl groups. The CYS and PEI ligands produce small hydrodynamic diameter QDs (15–26 nm) with strong positive charge (+29 to +35 mV) due to the presence of amine groups that are protonated at pH=6.6. DTT produces a small hydrodynamic diameter (<10 nm) QD that is near neutral charged due to the high pKa of the hydroxyl groups. The hydration sphere surrounding the QD depends on surface charge and therefore slightly larger HDs are measured for the highly charged QDs. Based on the absorption, fluorescence emission, size, and surface charge data we can conclude that the water soluble QDs are well dispersed and the core size unchanged.

Quantum yields of QDs coated with different ligands were measured relative to Rhodamine 6G with excitation at 488 nm (Table 2). Results show that positive PEI-coated QDs and negative GSH-coated QDs exhibit the highest QY of 53.3% and 40.7%, respectively, which

nearly as efficient as the organic coated QDs (56%). The ligand dependent QY values are consistent with the variation in peak PL intensity (Fig. 2).

## Long-term stability of QDs

One figure-of-merit used to assess the quality of water soluble coating is to examine long-term stability of QDs. We measured the mean particle size and zeta potential of QDs stored at 4 °C in a dark place for 18 months. The average mean particle size and the zeta potential of all QDs, excluding DTT-QD and CYS-QD, remained extremely constant throughout the storage period yielding size and charge values consistent with those listed in Table 2. In addition, the stability of QDs stored at room temperature in dark place was also examined. All QDs except PEI-QD formed aggregation in 90 days. These results suggest that (1) multivalent polymeric ligands such as PEI make more stable QDs than small (low MW) ligands which presumably are more liable, (2) negative charged QDs produced with small ligands are more stable than positive or neutral QDs produced with small ligands, and (3) QD stability is temperature dependent. Stability is improved with storage under cool and dark conditions.

## Determination of ROS generation for different ligands capped QDs in HaCaT cells using flow cytometry

As a means to assess cytotoxicity we quantified oxidative stress in HaCaT cells, a normal keratinocyte cell line, following exposure to the different ligand capped QDs. Relative levels of reactive oxygen species (ROS) were quantified using the standard DCF-DA assay in which the magnitude of the fluorescence signal in the cells was determined using flow cytometry. A plot of the mean fluorescent intensity (Figure 4A, n=3) shows the highest ROS production results from exposure to the positive charged PEI capped QDs. Figure 4B shows a direct comparison of the fluorescence intensity histograms for one HaCaT cell sample exposed to negative charge GSH-QDs (dash line) and DHLA-QDs (solid line). Results show that DHLA-QDs produce higher ROS levels than GSH-QDs. Figure 4C show a comparison of the fluorescence intensity histogram illustrating ROS differences in HaCaT cells exposed to CYS-QDs (dash line) and PEI-QDs (solid line). Results show that PEI-QDs produce significantly higher ROS levels than CYS-QDs.

## Determination QD cellular association using flow cytometry

Flow cytometry was also used to quantify the QD cellular association. Figure 5A shows comparison of mean QD fluorescence intensity for HaCaT cells (n=3) exposed to the different ligand capped QDs corrected for autofluorescence measured in control cells (no QD exposure). Results clearly show that the positively charged PEI-QDs and CYS-QDs interact with cells to a much greater extent than the negative charge QDs. This is consistent with expectations as positive charged QDs should have greater affinity to interact electrostatically with the negatively charged glycocalyx on cell membranes[34]. Figure 5B shows a direct comparison of the fluorescence histogram for the negative charged DHLA and GSH capped QDs. Results suggest a slightly weaker interaction of GSH-QDs with HaCaT cells compared to DLHA-QDs. Figure 5C shows comparison of the positive charged CYS and PEI capped QDs. It is clear that the cellular association of PEI-QD far exceeds that of CYS-QD. It is of interest to note however, that despite the high cellular association of

CYS-QD, the ROS response is considerable less than that generated from PEI-QD (Fig. 4). This suggests a possible difference in the mechanisms by which QDs are processed by the cells which is dependence on ligand composition. Detailed studies of ligand dependent cellular uptake and processing are on-going.

### QD association assessed by fluorescence microscopy

Fluorescent microscope images of HaCaT cells in culture were taken following 24 h exposure QD and washing. Figure 6 show images for GSH-, DHLA-, CYS-, PEI coated QDs. Results are qualitatively consistent with the quantitative ROS and flow cytometry data showing that cellular association with positively charged QDs (PEI-QD, CYS-QD) is significantly higher than the negatively charged QDs (GSH-QD, DHLA-QD).

### Cell Viability Study by MTT Assay

MTT is a common assay used to measure mitochondrial enzyme activity and is thus an indirect measure of cell viability. The MTT assay has been used to quantify the cytotoxicity of various types of QDs and cell types[22,24,35]. Flow cytometry results and fluorescent microscope images suggest that cationic QDs interact with HaCaT cells more than negative QDs and that PEI-QD induce highest levels of ROS. It is expected that positive charged QDs will have greater affinity to interact with the negatively charged cell membranes[34]. The increased levels of oxidative stress associated with PEI-QD exposure suggest greater cell membrane disruption. To evaluate this we quantified the cytotoxicity dependence on QDs coating chemistry using the standard MTT assay for similar charged QD. Figure 7 shows cell viability data obtained from positive (PEI, CYS) and negative (GSH, DLHA) QDs exposed to HaCaT cells at the same molar concentration (10 nM) relative to a control (no QDs). The results show that the PEI-coated dots are the most toxic and the GSH-coated dots show no toxicity over the time course and dose studied. This data confirms that ligand composition in addition physicochemical properties[21,28] impacts cytotoxicity. GSH is a natural tripeptide (γ-L-glutamyl-L-cysteinylglycine) that exists in most tissues. It is a natural antioxidant that cells use to prevent damage from ROS. Although detailed cellular processing studies are in progress, our data provides further support that cells are able to recognize and respond to the composition of the ligands coated on QD. These findings corroborate previous studies investigating the cytotoxicity of commercially available (Invitrogen) polyethylene glycol (PEG), PEG-amine, and carboxylic acid coated QDs toward primary epidermal keratinocytes[22]. Using the MTT assay this study showed cytotoxicity was dependent on QD coating and time. Only carboxylic acid coated QDs (20 nM) exhibited detectible cytotoxicity after 24 hr exposure. After 48 hrs all three QD types exhibited statistically significant cytotoxicity. QD cell uptake was qualitatively examined by laser scanning confocal microscopy and TEM was determined to be independent of surface coating which is in contrast to quantitative results we observe using flow cytometry. We find that cytotoxicity and QD uptake are both dependent on surface coating composition.

## Conclusions

The ideal nanoparticle for biomedical imaging applications should be chemically and physically stable in the biological milieu – no oxidation, aggregation, agglomeration or

toxicity. Nanoparticles used for biomolecular fluorescent imaging would also have high quantum yield. In this study we undertook the design of QD nanoparticles with positive, negative and neutral surface charge to identify ligand coatings that exhibit the optimum properties of high stability, high QY and low cytotoxicity. Simple protocols are described to prepare water soluble QD by modifying the surface with thiol containing ligands and polymers. The results suggest that negative charged GSH coated QDs show superior performance exhibiting low cytotoxicity, high stability, high QY and therefore are best suited for use in bioimaging applications. PEI coated QDs also show superior performance exhibiting high QY and stability but they were highly cytotoxic and therefore may be advantageous for tumor imaging and targeting applications[36–37]. PEI coatings on various types of NPs have been widely investigated as nonviral transfection agents coated for gene and drug delivery to cells[38–40]. The positive PEI charge binds negatively charged oligoneuclotides and the negatively charged cell membrane[34]. Studies suggest that the PEI molecular weight, degree of branching and NP aggregation can be tuned to minimize cytotoxicity and enhance transfection efficacy[38–40]. The high cytotoxicity observed in our study is expected based on the highly branched and high MW PEI used. Studies investigating the mechanistic details of cellular uptake and processing of our QDs are on-going. The synthetic procedures described are extraordinary simple and can be easily adapted in most laboratory settings.

## Methods

### A) Materials

Commercial CdSe/ZnS octadecylamine (ODA)-capped QDs with emission at 620 nm and core/shell diameter of 6.2 nm (NN-Labs, Fayetteville, AR) were used in this study. Glutathione (GSH, 98%), N-acetylcysteine (NAC, 99%), thioctic acid (98%), tiopronin (TP, 99%), cysteamine hydrochloride (CYS, 98%), mercaptosuccinic acid (MSA, 98%), 1,4-dithiothreitol (DTT, 98%), polyethylenimine (PEI, MW 25,000) and tetramethylammonium hydroxide (99%) were purchased from Sigma-Aldrich. Bucilliamine (BUC, 98%) was purchased from Shanghai Rainbow Chemistry Co. Ltd (China). Organic solvents used were of analytical reagent grade.

### B) Preparation of Water Soluble QDs

**B1) Synthesis of Dihydrolipoic acid (DHLA)—**DHLA (yellowish oil) was freshly prepared through the deoxidation of thioctic acid by $NaBH_4$ following established procedures[41–43]. Briefly, to 19.5 mL of a 0.25 M $NaHCO_3$ solution containing 1.0 g of thioctic acid, a total of 0.2 g of $NaBH_4$ was added slowly. The mixture was vigorously stirred and kept in a cold bath (0–5 °C) (Fig. 4SA) After 2 h, 16.7 mL of toluene was added and a two-phase solution resulted. The solution was acidified to pH 1 with HCl solution. The reduced thiotic acid was fully into the organic phase resulting in a whitish milky appearance (Fig. 4SB). The organic phase containing the reduced thiotic acid was collected and dried over an excess of anhydrous $MgSO_4$ (Fig. 4SC). The organic solvent was removed using a rotovap and 0.9 g DHLA was produced (yield 90 %), (Fig. 4SD).

**B2) Preparation of negatively charged CdSe/ZnS QDs with thiol-based ligands**
—The QDs in organic solvent (toluene, 5 mg/mL) were precipitated by addition to a (1:1)
methanol: acetone solution. The organic QDs (0.25 μM, 200 μL) were added to ~1 mL
methanol:acetone and separated by centrifugation at 14,000 rmp for 5 min. The QD pellet
was redissolved in 200 μL tetrahydrofuran (THF). Transferring QD into THF is a preferable
over decane, hexane, or chloroform for solublizing the organic ligand following exchange.
Negatively charged QDs were prepared by ligand exchange with bifunctional GSH, NAC,
DHLA, TP, MSA or BUC (Table 1) using the procedure described below. The thiol-based
ligand (~20 mg) was added to 1 mL methanol. The pH of the ligand solution was adjusted to
11 with tetramethylammonium hydroxide pentahydrate ($(CH_3)_4NOH\cdot5H_2O$) powder. The
QD THF solution was then slowly added to the ligand solution at room temperature. The
ligand concentration was chosen to be ~$10^6$ molar excess to the QD. The mixture was stirred
at 60 °C for 2 h (Figure 5SA) and the QD precipitated with the addition of ether (1–2 mL,
J.T. Baker, NJ) by centrifugation at 14,000 rmp for 5 min (Figure 5SB). The supernatant
was discarded and the QD pellet was redispersed in deionized water (100μL) (Figure 5SC).
The QDs were dialyzed using a 5 kD molecular weight cutoff DispoDialyzer filter (Harvard
Apparatus Inc.) in 500x excess volume of water for 72 hours with water changes every 24
hours. After dialyzing, the QD concentration was determined by measuring the absorption at
the first excitation and using an extinction coefficient from the literature with Lambert-
Beer's law[44].

**B3) Preparation of positive charged CdSe/ZnS QDs with thiol-based ligands**—
Amino-CdSe/ZnS QDs (CYS-QDs) were synthesized according to a previously reported
method[45]. Briefly, cysteamine hydrochloride (50 mg) was added to 2.0 mL capped vial and
heated at 80°C (~10 min). After melting, the QD THF solution (0.25 μM, 200 μL), prepared
as described in section B2, was added drop wise to the vial while still hot. The vial was
recapped and heated at 80°C for 2h. The sample was flushed with $N_2$ stream to remove
organic solvent. The product appeared as sticky solid which was then dissolved using
deionized water (100 μL). The QDs are dialyzed using a 5kD molecular weight cutoff
DispoDialyzer filter (Harvard Apparatus Inc.) and 500x excess volume of water for 72 hours
with water changing every 24 hours. After dialyzing, the QD concentration was determined
by measuring the absorption at the first excitation and using an extinction coefficient from
the literature with Lambert-Beer's law[44].

**B4) Preparation of neutral charged CdSe/ZnS QDs with thiol-based ligands**—
Hydroxyl-CdSe/ZnS QDs (DTT-QDs) were synthesized with dithiothreitol (DTT) by a thiol
exchange method[46]. Briefly, DTT (20 mg) was added to methanol (1 mL) and the pH of the
solution was adjusted to 8–9 with tetramethylammonium hydroxide pentahydrate
($(CH_3)_4NOH \cdot 5H_2O$). DTT methanol solution was slowly added to the QD THF solution
(0.25 μM, 200 μL) prepared as described in section B2. The mixture was stirred overnight at
room temperature and precipitated with the addition of ether by centrifugation at 14,000 rmp
for 5 min. The supernatant was discarded and the QD sample was redispersed in deionized
water (100 μL). The QDs were dialyzed using a 5 kD molecular weight cutoff
DispoDialyzer filter (Harvard Apparatus Inc.) and 500x excess volume of water for 72 hours
with water changing every 24 hours. After dialyzing, the concentration is determined by

measuring the absorption at the first excitation and using an extinction coefficient from the literature with Lambert-Beer's law[44].

**B5) Preparation of positive charged CdSe/ZnS QDs with hyperbranched polyethylenimine ligand—**Positively charged amino-capped CdSe/ZnS QDs were synthesized through direction ligand-exchange reaction with hyperbranched polyethylenimine ligand (PEI-QDs)[47]. Briefly, the PEI (Mw = 25 kD, branched) was first dissolved in THF at a concentration of 80 mg/ml. PEI THF solution (500 μL) was slowly added to the QD THF solution (0.25 μM, 400 μL) prepared as described in section B2. The mixture in a capped vial was stirred overnight at room temperature. The sample was flushed with a $N_2$ stream to remove the bulk of the organic solvent. The product appeared as sticky semisolid which was then washed and vortexed twice with excess THF to remove residual PEI. Residual THF was removed by ultrafiltration 14,000 rmp for 5 min using a nanosep 3 K filter (Pall Life Sciences, MI) and the product was resuspended in deionized water (100 μL). After ultrafiltration, the concentration is determined by measuring the absorption at the first excitation and using an extinction coefficient from the literature with Lambert-Beer's law[44].

## C) Characterization of QDs

**C1) Optical Characterization—**UV/Vis absorption spectra were measured at room temperature with a Shimadzu UV-1601PC photometer Unit (Shimadzu Scientific Instruments, Inc. Columbia, MD, USA) and photoluminescence (PL) spectra were collected with a modular Acton Research fluorometer equipped with a Ge detector, respectively. PL spectra were taken at the excitation wavelength λex = 488nm and at the excitionic aborption peak for PL quantum yields. Rhodamine 6G was used as a standard for determining PL quantum yield (QYs). Solution concentration of the various QD types was 8 μM.

**C2) Transmission electron microscopy (TEM)—**We examined the size and the morphology of the CdSe/ZnS QDs by transmission electron microscopy (TEM) using a Hitachi H-7100 with 1 drop of the ODA-QD solution mounted on a thin film of amorphous carbon deposited on a copper grid.

**C3) Hydrodynamic size measurements—**Hydrodynamic size of QD was evaluated by using hydrodynamic size (DLS). DLS measurements were performed using a Malvern Nano-ZS zetasizer (Malvern Instruments Ltd, Worcestershire, United Kingdom). The Nano-ZS employs non-invasive back scatter (NIBS™) optical technology and measures real time changes in intensity of scattered light as a result of particles undergoing Brownian motion. The sample is illuminated by a 633 nm Helium-Neon laser and the scattered light is measured at an angle of 173° using an avalanche photodiode. The size distribution of the vesicles is calculated from the diffusion coefficient of the particles according to Stokes-Einstein equation. The average diameter and the polydispersity index of the samples are calculated by the software using CONTIN analysis.

**C4) Zeta potential measurements—**The zeta potential of QD was measured with the Malvern Nano ZS using the technique of Laser Doppler Velocimetry (LDV). In this

technique, a voltage is applied across a pair of electrodes at either end of the cell containing the particle dispersion. Charged particles are attracted to the oppositely charged electrode and their velocity was measured and expressed in unit field strength as an electrophoretic mobility. The zeta potential was calculated from the electrophoretic mobility using Henry's equation.

**C5) Stability of QDs in aqueous solution**—The physical stability of QDs was evaluated. Briefly, deionized water aqueous solution of QDs was preserved in the dark at 4 °C and room temperature for 18 months Hydrodynamic size and zeta potential of QDs were measured using DLS.

## D) Treatment of Cells with QDs

**D1) Cell line**—The human keratinocytes cell line HaCaT was obtained from ATCC and cultured in high-glucose Dulbecco's modified Eagle's medium (DMEM). Media contained 10 % fetal calf serum, streptomycin (1mg /mL) and penicillin (1000 units /mL). All cells were cultured at 37°C in water-saturated air supplemented with 5% $CO_2$. Culture media were changed every three days. Cells were passaged once a week. Cells in the exponential growth phase were used for experiment.

**D2) Flow cytometric determination of oxidative stress and QDs uptake**— HaCaT cells were plated in 12-well plates and then incubated up to about 48 h and grow to about 80% confluence before experiments. The medium was replaced by DMEM (1.5 mL) containing 10 nM of GSH-, NAC-, TP-, BUC-, DHLA-, MSA-, CYS-capped QDs, and cells were incubated for 24 hrs at 37°C, followed by staining with 10 μM 2',7'-dichlorodihydrofluorescein diacetate (DCF-DA, Invitrogen, Grand Island, NY) for 30 min at 37°C. The cells were then trypsinized with 0.25% trypsin-EDTA. The samples were then centrifuged and the pellet fixed in 3% Formalin. Appropriate controls and single-stain controls for compensation were included in each experiment. 20,000 cells were analyzed by using BD LSR II flow cytometry (Becton–Dickinson) at an excitation wavelength of 488 nm and emission wavelengths of 515 for DCF-DA, at an excitation wavelength of 405 nm and emission wavelengths of 605 for fluorescence profile of the QD- associated cells, respectively. Results from flow cytometry were analyzed using the Flow Jo (Version 7.5) software.

**D3) Fluorescence spectrophotometry assessment of QDs ROS**—HaCaT cells were plated in 12-well plates and then incubated up to about 48 h and grow to about 50% confluence before experiments. The medium was replaced by DMEM (1.5 mL) containing 10nM of GSH-, DHLA-, CYS-, PEI-capped QDs, and cells were incubated for 24 hrs at 37 °C, followed by staining with 10 μM 2',7'-dichlorodihydrofluorescein diacetate (DCF-DA, Invitrogen, Grand Island, NY) for 30 min at 37 °C. At the end of the incubation, the medium was removed. The cells were fixed in 3% Formalin and finally analyzed under a fluorescence microscope (Olympus IX70 with QImaging Retiga EXi camera) at 40x magnification with pictures obtained under bright field and fluorescent filters (DCF-DA, excitation 480 nm/emission 510 nm; QD, excitation 360 nm/emission 620 nm). Images were analyzed using ImageJ.

**D4) Cell viability (MTT assay) of QDs**—HaCaT cells were plated in 96-well plates and grown to about 50% confluence. The culture medium was removed, and replaced with media containing 10 nM of GSH-, DHLA-, CYS-, PEI-capped QDs. After incubation for 24hr, media was removed and replaced by 100 μL of the MTT (5 mg/mL MTT dissolved in PBS) solution per well and the plates were incubated for 5 hr. Thereafter, the media was replaced with 0.4 mL of acidic isopropyl alcohol (0.04 M HCl in absolute isopropyl alcohol) to solubilize the colored formazan crystals. The absorbance of the resulting solutions was read at 600 nm wavelength in microplate reader.

## Supplementary Material

Refer to Web version on PubMed Central for supplementary material.

## Acknowledgments

## References

1. Chan WC, Nie S. Quantum dot bioconjugates for ultrasensitive nonisotopic detection. Science. 1998; 281:2016–2018. [PubMed: 9748158]

2. Bruchez M Jr, Moronne M, Gin P, Weiss S, Alivisatos AP. Semiconductor nanocrystals as fluorescent biological labels. Science. 1998; 281:2013–2016. [PubMed: 9748157]

3. Wang DS, He JB, Rosenzweig N, Rosenzweig Z. Superparamagnetic $Fe_2O_3$ Beads-CdSe/ZnS quantum dots core-shell nanocomposite particles for cell separation. Nano Lett. 2004; 4:409–413.

4. Dahan M, Lévi S, Luccardini C, Rostaing P, Riveau B, Triller A. Diffusion dynamics of glycine receptors revealed by single-quantum dot tracking. Science. 2003; 302:442–445. [PubMed: 14564008]

5. Trindade T, O'Brien P, Pickett NL. Nanocrystalline Semiconductors. Synthesis, Properties, and Perspectives Chem Mater. 2001; 13:3843–3858.

6. Talapin DV, Rogach AL, Kornowski A, Haase M, Weller H. Highly Luminescent Monodisperse CdSe and CdSe/ZnS Nanocrystals Synthesized in a Hexadecylamine Trioctylphosphine Oxide Trioctylphospine Mixture. Nano Lett. 2001; 1:207–211.

7. Dabbousi BO, Rodriguez-Viejo J, Mikulec FV, Heine JR, Mattoussi H, Ober R, Jensen KF, Bawendi MG. (CdSe). ZnS Core Shell Quantum Dots: Synthesis and Characterization of a Size Series of Highly Luminescent Nanocrystallites. J Phys Chem B. 1997; 101:9463–9475.

8. Fan H, Leve EW, Scullin C, Gabaldon J, Tallant D, Bunge S, Boyle T, Wilson MC, Brinker CJ. Surfactant-Assisted Synthesis of Water-Soluble and Biocompatible Semiconductor Quantum Dot Micelles. Nano Lett. 2005; 5:645–648. [PubMed: 15826102]

9. Wuister SF, Swart I, van Driel F, Hickey SG, de Mello Donega C. Highly Luminescent Water-Soluble CdTe Quantum Dots. Nano Lett. 2003; 3:503–507.

10. Oh JK. Surface modification of colloidal CdX-based quantum dots for biomedical applications. J Mater Chem. 2010; 20:8433–8445.

11. Blanco-Canosa JB, Medintz IL, Farrell D, Mattoussi H, Dawson PE. Rapid Covalent Ligation of Fluorescent Peptides to Water Solubilized Quantum Dots. J Am Chem Soc. 2010; 132:10027–10033. [PubMed: 20597509]

12. Liu L, Guo X, Li Y, Zhong X. Bifunctional Multidentate Ligand Modified Highly Stable Water-Soluble Quantum Dots. Inorg Chem. 2010; 49:3768–3775. [PubMed: 20329710]

13. Gerion D, Pinaud F, Williams SC, Parak WJ, Zanchet D, Weiss S, Alivisatos AP. Synthesis and properties of biocompatible water-soluble silica-coated CdSe/ZnS semiconductor quantum dots. J Phys Chem B. 2001; 105:8861–8871.

14. Pellegrino T, Manna L, Kudera S, Liedl T, Koktysh D, Rogach AL, Keller S, Radler J, Natile G, Parak WJ. Hydrophobic nanocrystals coated with an amphiphilic polymer shell: A general route to water soluble nanocrystals. Nano Lett. 2004; 4:703–707.

15. Dubertret B, Skourides P, Norris DJ, Noireaux V, Brivanlou AH, Libchaber A. In vivo imaging of quantum dots encapsulated in phospholipid micelles. Science. 2002; 298:1759–1762. [PubMed: 12459582]

16. Choi HS, Liu W, Misra P, Tanaka E, Zimmer JP, Ipe BI, Bawendi MG, Frangioni JV. Renal clearance of quantum dots. Nat Biotechnol. 2007; 25:1165–1170. [PubMed: 17891134]

17. Cho SJ, Maysinger D, Jain M, Roder B, Hackbarth S, Winnik FM. Long term exposure to CdTe quantum dots causes functional impairments in live cells. Langmuir. 2007; 23:1974–1980. [PubMed: 17279683]

18. Choi AO, Cho SJ, Desbarats J, Lovri J, Maysinger D. Quantum dot-induced cell death involves Fas upregulation and lipid peroxidation in human neuroblastoma cells. J Nanobiotechnology. 2007; 5:1. [PubMed: 17295922]

19. Choi AO, Brown SE, Szyf M, Maysinger D. Quantum dot-induced epigenetic and genotoxic changes in human breast cancer cells. J Mol Med. 2008; 86:291–302. [PubMed: 17965848]

20. Lovri J, Cho SJ, Winnik FM, Maysinger D. Unmodified cadmium telluride quantum dots induce reactive oxygen species formation leading to multiple organelle damage and cell death. Chem Biol. 2005; 12:1227–1234. [PubMed: 16298302]

21. Hoshino A, Fujioka K, Oku T, Suga M, Sasaki YF, Ohta T, Yasuhara M, Suzuki K, Yamamoto K. Physicochemical properties and cellular toxicity of nanocrystal quantum dots depend on their surface modification. Nano Lett. 2004; 4:2163–2169.

22. Ryman-Rasmussen JP, Riviere JE, Monteiro-Riviere NA. Surface coatings determine cytotoxicity and irritation potential of quantum dot nanoparticles in epidermal keratinocytes. J Inves Dermatol. 2007; 127:143–153.

23. Chang E, Thekkek N, Yu WW, Colvin VL, Drezek R. Evaluation of quantum dot cytotoxicity based on intracellular uptake. Small. 2006; 2:1412–1417. [PubMed: 17192996]

24. Hardman R. A toxicologic review of quantum dots: toxicity depends on physicochemical and environmental factors. Environ Health Perspect. 2006; 114:165–172. [PubMed: 16451849]

25. Choi, AO.; Maysinger, D. Semiconductor Nanocrystal Quantum dots Synthesis, Assembly, Spectroscopy and Application. Rogac, A., editor. Springer; 2008. p. 348-367.

26. Nann T. Phase-transfer of CdSe-ZnS quantum dots using amphiphilic hyperbranched polyethylenimine. Chem Commun. 2005; 7:1735–1736.

27. Wisher AC, Bronstein I, Chechik V. Thiolated PAMAM dendrimer-coated CdSe/ZnSe nanoparticles as protein transfection agents. Chem Commun (Camb). 2006; 15:1637–1639. [PubMed: 16583004]

28. Lovriæ J, Bazzi HS, Cuie Y, Fortin GR, Winnik FM, Maysinger D. Differences in subcellular distribution and toxicity of green and red emitting CdTe quantum dots. J Mol Med. 2005; 83:377–385. [PubMed: 15688234]

29. Deneke SM. Thiol-based antioxidants. Curr Top Cell Regul. 2000; 36:151–180. [PubMed: 10842751]

30. Hayase Y, Fukatsu H, Segawa A. Dissolution of cystine stones by irrigated tiopronin solution. J Urol. 1980; 124:775–778. [PubMed: 7441827]

31. Mattoussi H, Mauro JM, Goldman ER, Anderson GP, Sundar VC, Mikulec FV, Bawendi MG. Self-Assembly of CdSe-ZnS Quantum Dot Bioconjugates Using an Engineered Recombinant Protein. J Am Chem Soc. 2000; 122:12142–12150.

32. Clapp AR, Goldman ER, Mattoussi H. Capping of CdSe-ZnS quantum dots with DHLA and subsequent conjugation with proteins. Nat Protoc. 2006; 1:1258–1266. [PubMed: 17406409]

33. Algar WR, Krull UJ. Luminescence and stability of aqueous thioalkyl acid capped CdSe/ZnS quantum dots correlated to ligand ionization. ChemPhysChem. 2007; 8:561–568. [PubMed: 17274093]

34. Fischer D, Li Y, Ahlemeyer B, Krieglstein J, Kissel T. In vitro cytotoxicity testing of polycations: influence of polymer structure on cell viability and hemolysis. Biomaterials. 2003; 24:1121–1131. [PubMed: 12527253]

35. Clift MJ, Varet J, Hankin SM, Brownlee B, Davidson AM, Brandenberger C, Rothen-Rutishauser B, Brown DM, Stone V. Quantum dot cytotoxicity in vitro: an investigation into the cytotoxic effects of a series of different surface chemistries and their core/shell materials. Nanotoxicology. 2011; 5(4):664–74. [PubMed: 21105833]

36. Chen B, Huang M-S, Yeh S, Kuo MYP, Hsiao M. Polyethylenimine Mediated Oral Cancer Targeted PUMA Gene Delivery Suppressed Tumor Growth and Prolonged Survival. Molecular Therapy. 2006; 13(1):S111.

37. Hildebrandt IJ, Iyer M, Wagner E, Gambhir SS. Optical imaging of transferrin targeted PEI/DNA complexes in living subjects. Gene Ther. 2003; 10(9):758–64. [PubMed: 12704414]

38. Xia T, Kovochich M, Liong M, Meng H, Kabehie S, George S, Zink JI, Nel Andre E. Polyethyleneimine Coating Enhances the Cellular Uptake of Mesoporous Silica Nanoparticles and Allows Safe Delivery of siRNA and DNA Constructs. ACS Nano. 2009; 3(10):3273–3286. [PubMed: 19739605]

39. Fischer D, Bieber T, Li Y, Elsässer HP, Kissel T. A novel non-viral vector for DNA delivery based on low molecular weight, branched polyethylenimine: effect of molecular weight on transfection efficiency and cytotoxicity. Pharm Res. 1999; 16(8):1273–9. [PubMed: 10468031]

40. Wang X, Zhou L, Ma Y, Li X, Gu H. Control of Aggregate Size of Polyethyleneimine-Coated Magnetic Nanoparticles for Magnetofection. Nano Res. 2009; 2:365–3729.

41. Roux S, Garcia B, Bridot JL, Salomé M, Marquette C, Lemelle L, Gillet P, Blum L, Perriat P, Tillement O. Synthesis, characterization of dihydrolipoic acid capped gold nanoparticles, and functionalization by the electroluminescent luminol. Langmuir. 2005; 21:2526–2536. [PubMed: 15752049]

42. Gunsalus IC, Borton LS, Gruber W. Biosynthesis and Structure of Lipoic Acid Derivatives. J Am Chem Soc. 1956; 78:1763–1766.

43. Wagner AF, Walton E, Boxer GE, Pruss MP, Holly FW, Folkers K. Properties and derivatives of lipoic acid. J Am Chem Soc. 1956; 78:5079–5081.

44. Yu WW, Qu L, Guo W, Peng X. Experimental determination of the extinction coefficient of CdTe, CdSe, and CdS nanocrystals. Chem Mater. 2003; 15:2854–2860.

45. Xiao Q, Zhou B, Huang S, Tian F, Guan H, Ge Y, Liu X, He Z, Liu Y. Direct observation of the binding process between protein and quantum dots by in situ surface plasmon resonance measurements. Nanotechnology. 2009; 20:325101. [PubMed: 19620762]

46. Pathak S, Choi SK, Arnheim N, Thompson ME. Hydroxylated quantum dots as luminescent probes for in situ hybridization. J Am Chem Soc. 2001; 123:4103–4104. [PubMed: 11457171]

47. Duan H, Nie S. Cell-penetrating quantum dots based on multivalent and endosome-disrupting surface coatings. J Am Chem Soc. 2007; 129:3333–3338. [PubMed: 17319667]
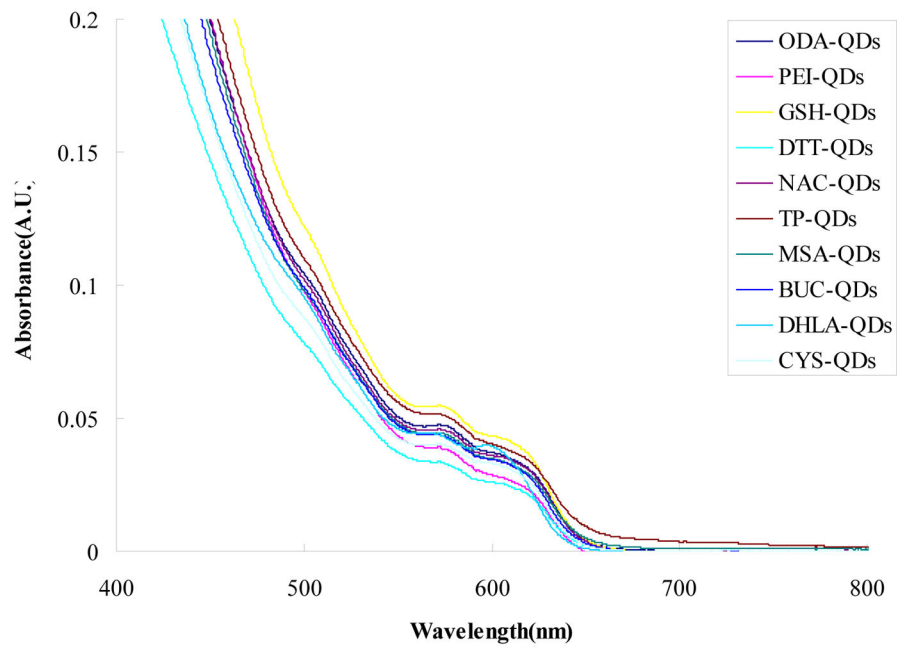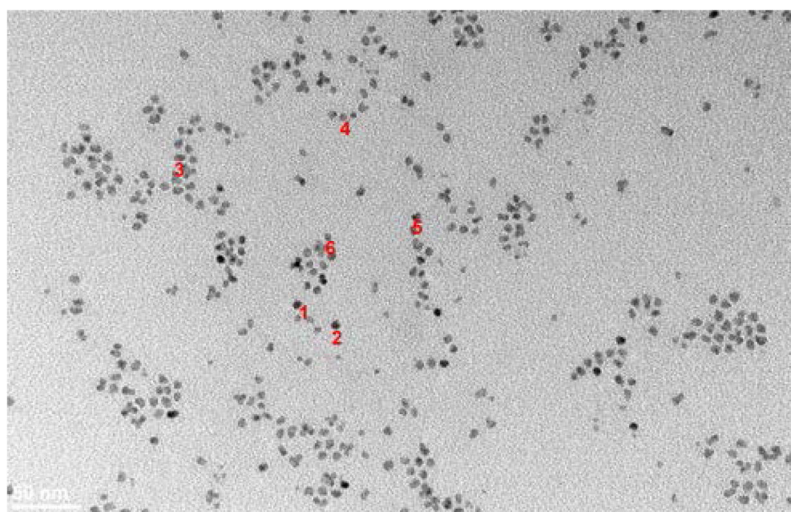
**Figure 1.**
Comparison of the UV/Vis absorption spectra for different ligands capped CdSe/ZnS QDs.
Solution concentration of the various QD types was 8 μM.
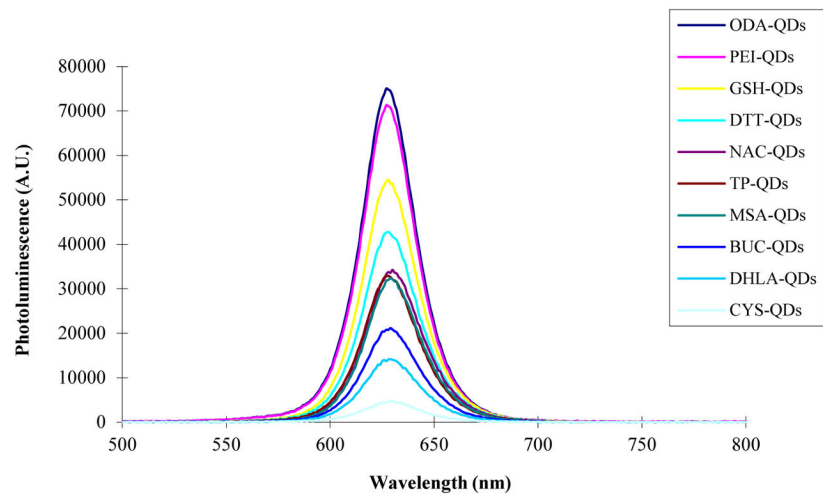
**Figure 2.**
Comparison of the photoluminescence (PL) spectra for different ligands capped CdSe/ZnS QDs. Solution concentrations of the various QD types was 8 μM.
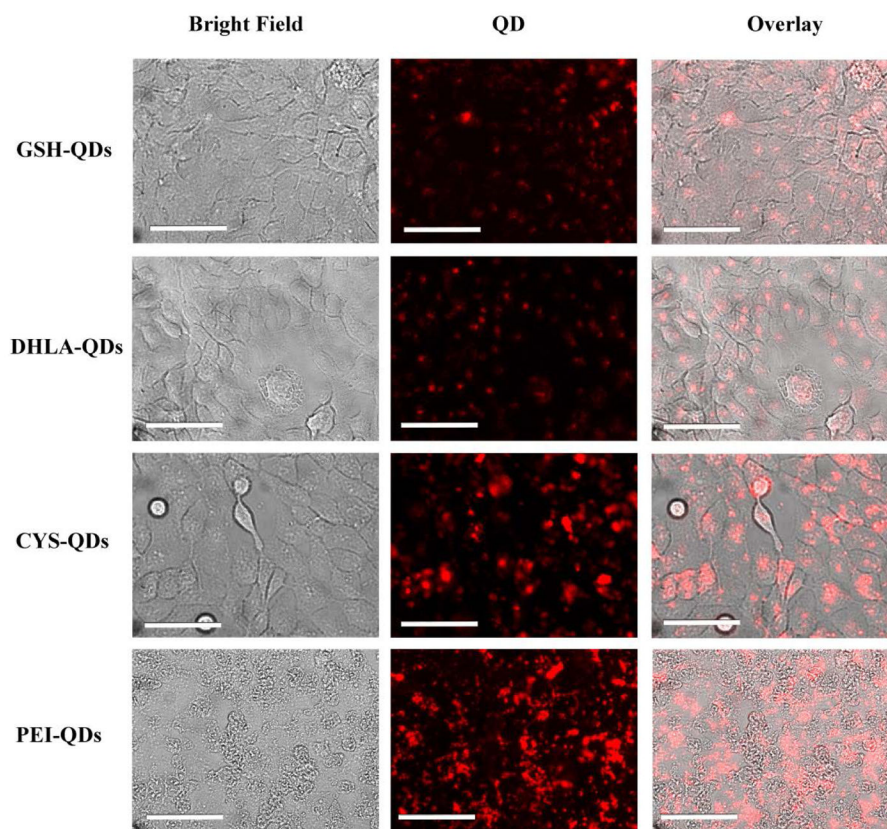
**Figure 3.**
Transmission electron micrographs of ODA-QDs in toluene.

Dot 1, diameteris : 6.57412nm

Dot 2, diameteris :6.59993nm

Dot 3, diameteris : 8.41729nm

Dot 4, diameteris :5.61882nm

Dot 5, diameteris, 7.03235nm

Dot 6, diameteris : 5.06439nm
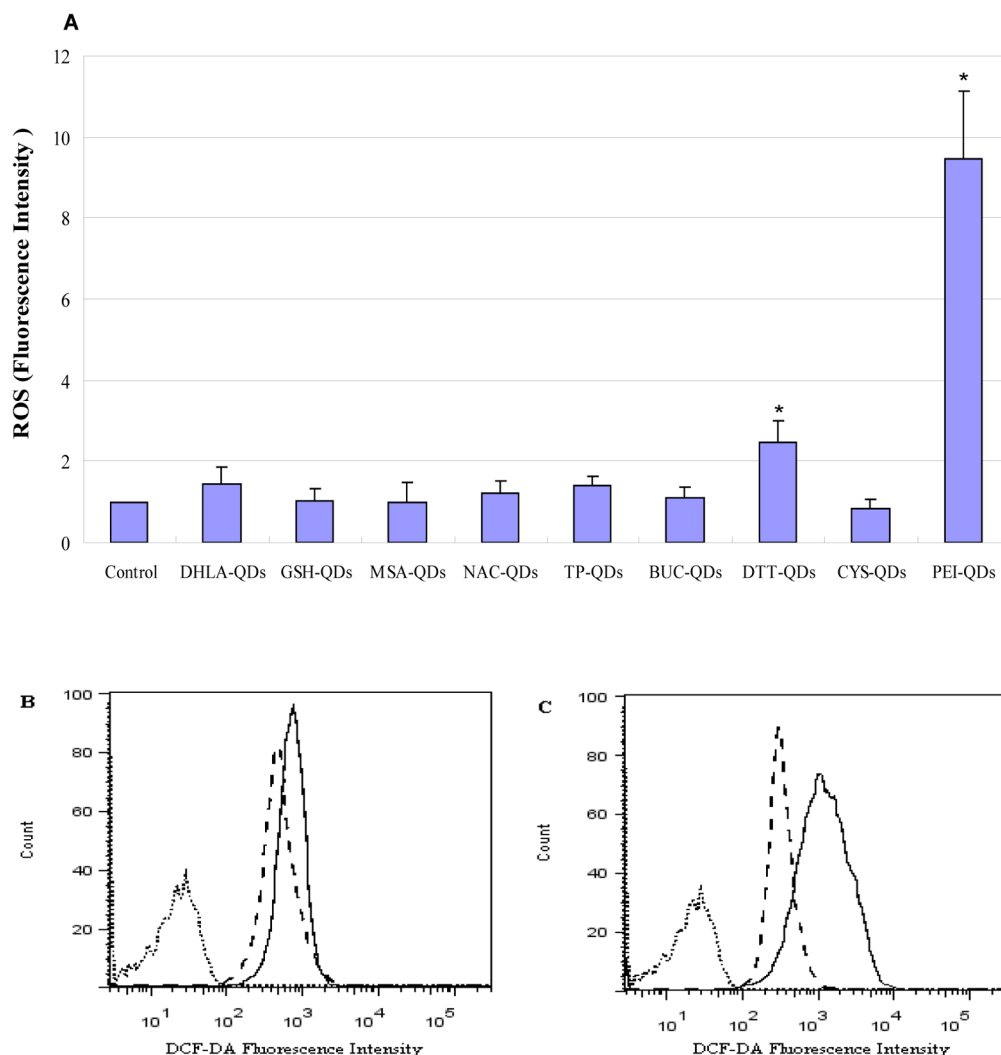
**Figure 4.**

(A) Comparison of ROS generation for different ligands capped QDs in HaCaT cells. ROS levels were determined by the DCF-DA as described in the Materials and Methods Section D. Cell cultures were treated with the different ligand capped QDs and ROS production was measured as fluorescence intensity. Results are expressed as mean fluorescence intensity value ±SD (n=3). * indicate significant differences between treated and untreated cell culture (*p*<0.05). (B) Fluorescence intensity histogram illustrating ROS differences in HaCaT cells exposed to GSH-QDs (dash line) and DHLA-QDs (solid line). Dotted line shows untreated cells. (C) Fluorescence intensity histogram illustrating ROS differences in HaCaT cells exposed to CYS-QDs (dash line) and PEI-QDs (solid line). Dotted line shows magnitude of autofluorescence from untreated cells.
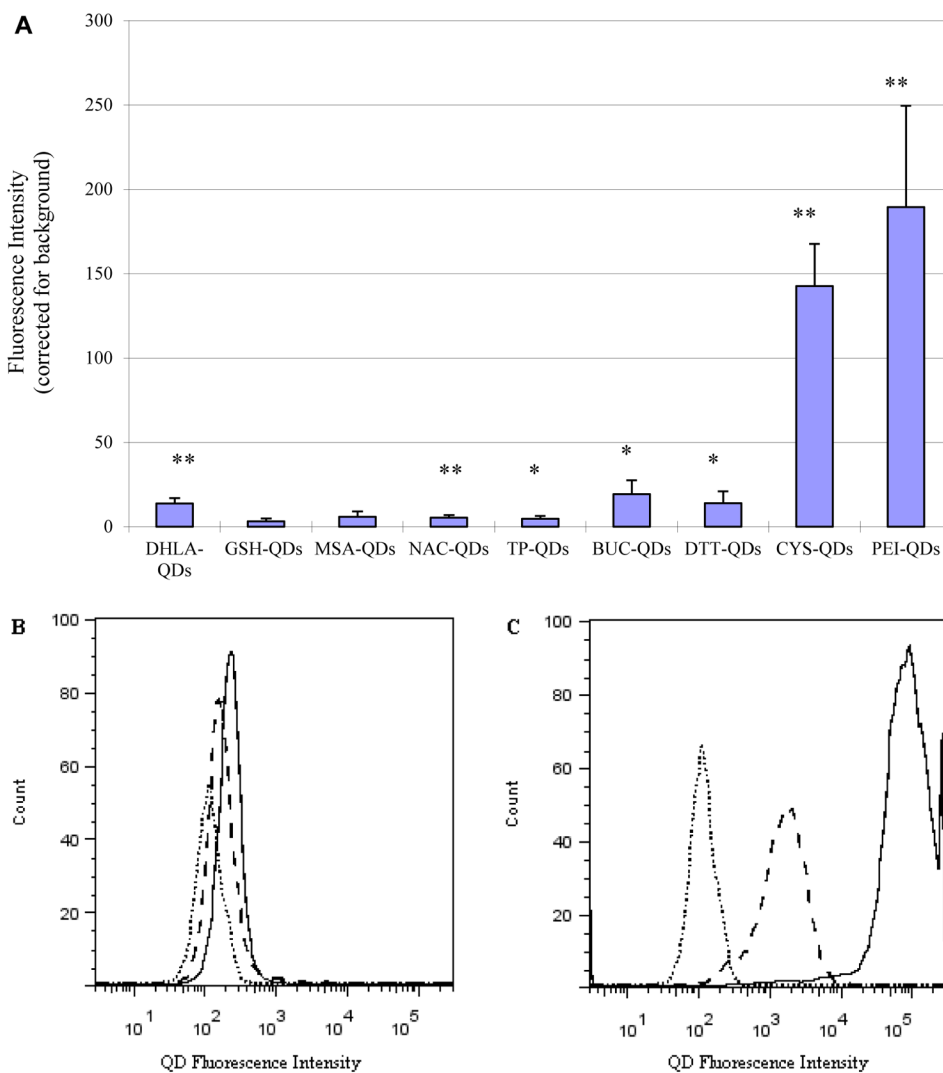
**Figure 5.**
(A) Comparison of QD HaCaT cell association with different ligand capped QDs (n=3). Data are expressed as mean fluorescence intensity units after subtracting autofluorescence background. Significance was * $p<0.05$, ** $p<0.005$. (B) Direct comparison of the fluorescence intensity histograms for HaCaT cells exposed to GSH-QDs (dash line) and DHLA-QDs (solid line). Dotted line shows untreated cells. Results suggest slightly greater interaction with DLHA-QD. (C) Direct comparison of the fluorescence intensity histograms for HaCaT cells exposed to CYS-QDs (dash line) and PEI-QDs (solid line). Dotted line shows untreated cells. Results suggest greater interaction with PEI -QD.

**Figure 6.**
Assessment of positive (CYS, PEI) and negative (GSH, DLHA) charged QDs interaction with HaCaT cell using fluorescence microscope following 24h incubation and washing. (Scale bar: 25μm)
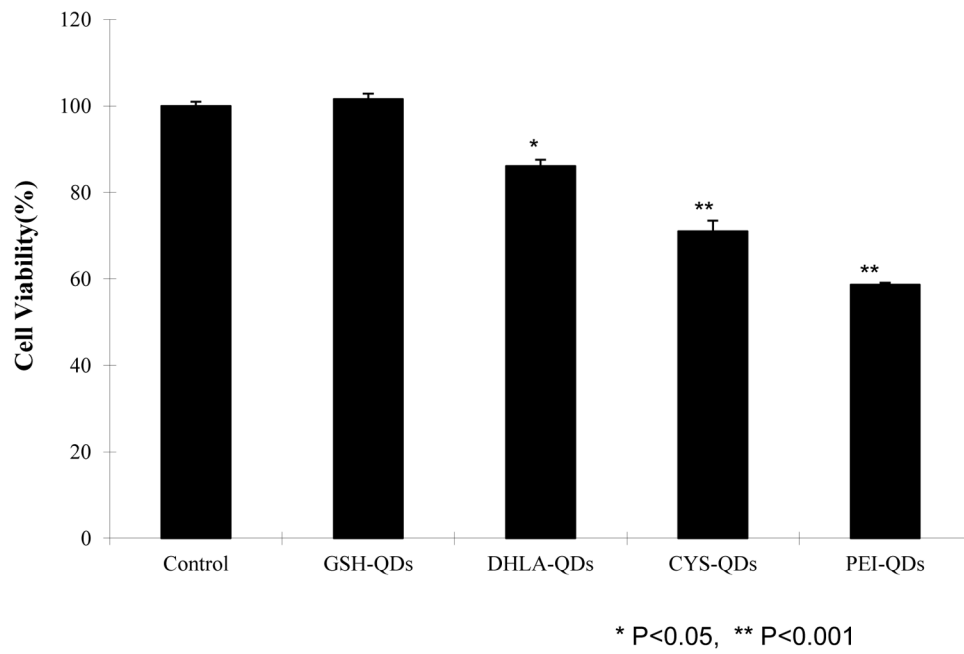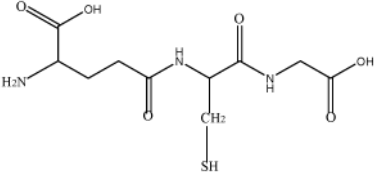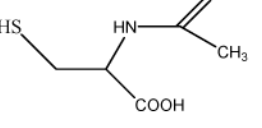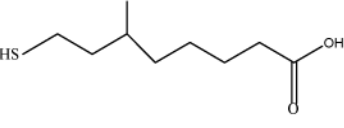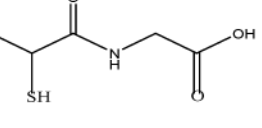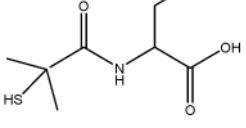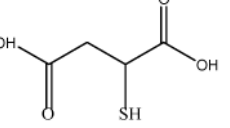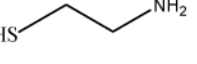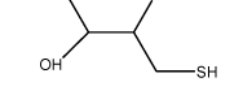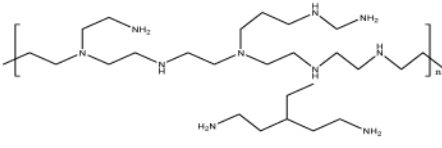
**Figure 7.**
HaCaT cell viability results for QDs coated with different ligands (10 nM) exhibiting both positive and negative charge obtained using standard MTT colorimetric assays (n=3).

**TABLE 1**

Structure and Molecular Weights ($M_W$) of the Ligands Used in This Work

| Name | Structure | Mw (g/mol) |
|------|-----------|------------|
| ODA |  | 269.51 |
| GSH |  | 223.32 |
| NAC |  | 163.19 |
| DHLA |  | 208.34 |
| TP |  | 163.19 |
| BUC |  | 223.31 |
| MSA |  | 150.15 |
| CYS |  | 77.15 |
| DTT |  | 154.25 |

| Name | Structure | Mw (g/mol) |
|------|-----------|------------|
| **PEI** |  | **25,000** |

**Table 2**

Comparison of size and surface-charge and Quantum yield of CdSe/ ZnS QDs with Different Ligands. Results are expressed as mean ± SD (*n=3*).

| Sample | Zeta potential [a] (mV) | Hydrodynamic diameter (nm) | Quantum yield (%) |
|--------|-------------------------|----------------------------|-------------------|
| ODA-QD | N/A | N/A | 56.0 |
| GSH-QD | −23.8±0.71 | 20.94±1.51 | 40.7 |
| NAC-QD | −35.3±1.82 | 28.09±1.20 | 25.8 |
| DHLA-QD | −26.2±7.18 | 13.63±0.71 | 10.6 |
| TP-QD | −34.17±1.00 | 23.85±2.88 | 24.9 |
| BUC-QD | −31.83±3.73 | 21.87±0.73 | 15.5 |
| MSA-QD | −35.3±1.65 | 28.15±2.74 | 23.9 |
| DTT-QD | −3.88±2.31 | 9.71±0.40 | 32.7 |
| CYS-QD | +35.27±0.25 | 15.66±0.95 | 6.5 |
| PEI-QD | +29.8±0.35 | 26.72±5.69 | 53.3 |

[a]Zeta potentials were measured within one week of synthesis placing 0.1mg/ mL of QDs in DI water, pH=6.6.